The Impact of IEEE 802.11 MAC Strategies on Multi-Hop Wireless Mesh Networks

Seongkwan Kim, Sung-Ju Lee, Sunghyun Choi
Mobile and Media Systems Laboratory
HP Laboratories Palo Alto
HPL-2006-135
September 29, 2006*

This paper analyzes the impact of different MAC (Medium Access Control) and transmission rate adaptation schemes on wireless mesh networks. The considered protocols include three different MAC protocols specified in IEEE 802.11 standards, i.e., 802.11, 802.11e, and 802.11n, and three rate adaptation schemes, i.e., ARF (Automatic Rate Fallback), RBAR (Receiver-Based Auto Rate), and 802.11n rate adaptation. We also study the interactions of these MAC strategies with the state-of-the-art routing metric ETT (Expected Transmission Time). Through comparative simulation evaluations, we investigate the effectiveness of these protocols when they coexist on both single-hop and multi-hop wireless mesh network environments. As these MAC strategies are designed for single-hop WLANs, we observed their limitations on multi-hop wireless mesh networks. We analyze their performances and suggest solutions for improvements. Based on our simulation results, we also argue for the need of a new routing metric that takes advantage of the new emerging MAC features.

The Impact of IEEE 802.11 MAC Strategies on Multi-Hop Wireless Mesh Networks

Seongkwan Kim
School of Electrical Engineering & INMC
Seoul National University
Seoul, 151-744, Korea
skim@mwnl.snu.ac.kr

Sung-Ju Lee
Mobile & Media Systems Lab
Hewlett-Packard Laboratories
Palo Alto, CA 94304
sjlee@hp.com

Sunghyun Choi
School of Electrical Engineering & INMC
Seoul National University
Seoul, 151-744, Korea
schoi@snu.ac.kr

Abstract— This paper analyzes the impact of different MAC (Medium Access Control) and transmission rate adaptation schemes on wireless mesh networks. The considered protocols include three different MAC protocols specified in IEEE 802.11 standards, i.e., 802.11, 802.11e, and 802.11n, and three rate adaptation schemes, i.e., ARF (Automatic Rate Fallback), RBAR (Receiver-Based Auto Rate), and 802.11n rate adaptation. We also study the interactions of these MAC strategies with the state-of-the-art routing metric ETT (Expected Transmission Time). Through comparative simulation evaluations, we investigate the effectiveness of these protocols when they coexist on both single-hop and multi-hop wireless mesh network environments. As these MAC strategies are designed for single-hop WLANs, we observed their limitations on multi-hop wireless mesh networks. We analyze their performances and suggest solutions for improvements. Based on our simulation results, we also argue for the need of a new routing metric that takes advantage of the new emerging MAC features.

I. Introduction

Wireless mesh networks have recently been gaining momentum and receiving interests from both research [1], [2] and deployment [3]–[8] sectors. Wireless mesh networking is an attractive solution for home, community, and enterprise networks as it is a self-configuring, instantly deployable, low-cost networking system. Wireless mesh network aims to provide reliable high throughput network connectivity to wireless users.

A wireless mesh network is composed of gateway nodes, mesh points, mesh access points, and wireless clients. Gateways connect the mesh network with the wired Internet. Mesh points, mesh access points, and gateways communicate with each other via wireless medium and form a wireless backbone network. Wireless clients gain network access by associating with a mesh access point. Recent research has focused on increasing the capacity of wireless backbone networks. Mobility and energy efficiency are of little concern in mesh backbones as mesh (access) points are stationary and power-plugged. Instead, the usage of multiple channels [9] and multiple radios [10] has been proposed to overcome the limited wireless capacity in multi-hop environments.

In this paper, we concentrate on techniques that work in single-radio, single-channel networks as well as multi-radio and multi-channels. Using simulations, we evaluate the performance of different channel access protocols specified in IEEE 802.11 standards (namely, 802.11 [11], 802.11e [12], and 802.11n [13]) and various transmission rate adaptation algorithms (namely, Automatic Rate Fallback [14], Receiver-Based Auto Rate [15], and 802.11n rate adaptation [13]) on various wireless mesh network scenarios. We study the interactions of channel access and rate adaptation by properly combining the two strategies. We analyze and discuss the limitations of protocols and algorithms in the wireless mesh environment and suggest ways to improve the performance.

Routing is also an important component in achieving high throughput wireless mesh networks. Metrics that represent wireless channel quality [16]–[18] are shown to perform better than traditional shortest-hops in wireless mesh settings [19]. These metrics are designed to work with 802.11 DCF, and it is not known how they coexist with emerging MAC (Medium Access Control) features. We use ETT (Expected Transmission Time) [17] as the route metric in our simulations and evaluate its performance with different MAC protocols.

The rest of the paper is organized as follows. Employed MAC/PHY (Physical Layer) standards and rate adaptation schemes are described in Section II and Section III, respectively. Section IV presents the routing metric we simulate in this paper. Simulation results and analysis are presented in Section V. The paper concludes with a summary and future work in Section VI.

II. MAC and PHY Standards

In this section, we discuss IEEE 802.11 MAC and PHY standards which are considered in the paper.

A. The 802.11 DCF

In the IEEE 802.11 standard, the DCF (Distributed Coordination Function) based on CSMA/CA (Carrier Sense Multiple Access with Collision Avoidance) is specified as a mandatory medium access scheme [11]. When a transmitter is ready to
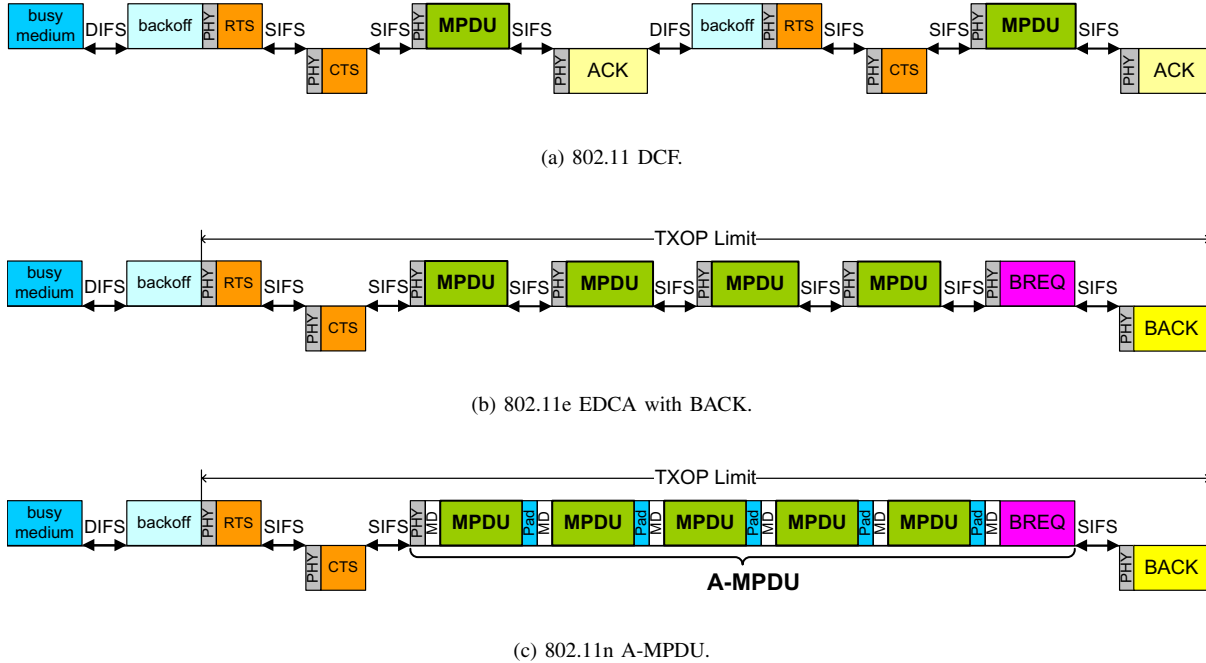
(a) 802.11 DCF.

(b) 802.11e EDCA with BACK.

(c) 802.11n A-MPDU.

Fig. 1. Medium access illustration of different schemes.

transmit a frame,[1] it checks the status of the channel. If the channel is busy, it waits until the end of the ongoing transmission. This part makes the DCF a CSMA protocol. When the channel becomes idle, instead of transmitting immediately, the transmitter selects a random backoff interval to reduce the collision probability. This part makes the DCF a collision avoidance protocol. If a data frame is successfully received, the receiver responds with an ACK (Acknowledgement) frame, after a SIFS (Short Inter-Frame Space) time interval. It is only after receiving an ACK frame correctly that the transmitter assumes a successful delivery of the corresponding data frame. On the other hand, if an ACK frame is received in error or no ACK frame is received, the transmitter assumes a failure of the corresponding data frame transmission. In this paper, such an ACK is referred to as *immediate ACK* to be differentiated from *BACK* (Block ACK) specified in IEEE 802.11e and IEEE 802.11n standards, which we describe later.

Fig. 1(a) illustrates frame exchange sequences of the DCF. In multi-hop environments, a frame exchange sequence with an RTS/CTS (Request-to-Send/Clear-to-Send) exchange is used to mitigate the hidden/exposed node problems. Nodes that overhear the duration field of RTS/CTS set their NAV (Network Allocation Vector) so that they do not interrupt a data transmission following the RTS/CTS exchange. The SIFS, which is the smallest time interval used between two consecutive frame transmissions, is used within this four-way – RTS-CTS-data-ACK – handshake. Other nodes must wait for

an idle medium for at least DIFS (DCF Inter-Frame Space) time interval, and hence are prevented from attempting to use the medium.

B. The 802.11e EDCA

IEEE 802.11e EDCA (Enhanced Distributed Channel Access) [12] enhances the DCF by providing differentiated and distributed channel accesses for frames with different user priorities. EDCA provides a new channel access method called *TXOP* (Transmission Opportunity). TXOP is a time interval when a particular transmitter has the right to initiate (multiple) frame exchange sequence(s) onto the wireless medium. A TXOP is defined by a starting time and a maximum duration (*TXOP limit*). During a TXOP, a node transmits one or more MPDUs[2] in a burst manner, separated by a SIFS.

BACK (Block ACK) is a new selective ARQ (Automatic Repeat reQuest) scheme defined in the 802.11e standard to improve the MAC efficiency. The scheme works as follows: during a TXOP, a transmitter can send a number of frames without receiving any immediate ACK. After all the frame transmissions are completed within the TXOP, the node transmits a *BREQ* (BACK Request). The receiving node of the

---

[1]In this paper, an 802.11 MPDU (MAC Protocol Data Unit) is referred to as a *frame*, while a *packet* is used to describe a network layer protocol data unit.

[2]In IEEE 802.11 standard, *x*PDU is defined as the unit of data exchanged between two peer entities using the service of the underlying protocol layer. Accordingly, *x*PDU becomes a *y*SDU (Service Data Unit) in the underlying protocol layer. For example, at the MAC layer, a MAC header and an MSDU (MAC Service Date Unit) compose an MPDU, and it in turn becomes a PSDU (PHY Service Data Unit) for the PHY.

TABLE I

MPDU DELIMITER.

MD fields	Size (bits)	Description
Reserved	4	
MPDU length	12	Length of the MPDU in octets
CRC	8	8-bit CRC of the preceding 16 bits
Unique pattern	8	Unique pattern that is used to detect an MD

BREQ responds with a BACK.[3] Fig. 1(b) shows the channel access of EDCA with BACK. *BACK bitmap* is used in BACK to inform which frames are not received correctly. BACK bitmap is the field inside the BACK frame, and a receiving node can acknowledge at most 64 MSDUs (MAC Service Date Units) at a time using the bitmap.

In order to protect the burst transmission during a TXOP from a possible collision, BACK should incorporate either an RTS/CTS exchange or an immediate ACK for the very first MPDU transmission in a TXOP. Otherwise, the whole bursting transmission during a TXOP could be corrupted in the worst case [20].

C. The 802.11n A-MPDU

The main objective of the ongoing IEEE 802.11n standardization is to develop a new MAC and PHY to significantly improve the throughput performance. It aims to provide a throughput of at least 100 Mbps as measured at the MAC SAP (Service Access Point), i.e., the interface between the MAC and the higher layer [13]. The 802.11n MAC is backward-compatible with the 802.11e MAC, which is in turn backward-compatible with the original 802.11 MAC. A-MPDU (Aggregate MAC Protocol Data Unit) and BACK, which we consider as representative MAC features of the 802.11n in this paper, are mandatory in the current 802.11n draft to constitute a high-efficient MAC protocol. Note that the BACK must be utilized in conjunction with A-MPDU in 802.11n, while the BACK is specified as an optional feature in the 802.11e standard.

A-MPDU frame aggregation is a MAC function and is architecturally done at the bottom of the MAC. When a transmitter with A-MPDU obtains a chance to transmit its frame(s), it searches MSDUs that are expected to be transmitted to the same receiver and have the same QoS (Quality of Service) requirement[4] from its MAC hardware queue. As illustrated in Fig. 1(c), an *MD* (MPDU Delimiter) and a *Pad* (padding octets) are attached in front and rear (except for a Pad field when it is the last aggregated packet) of an MPDU, respectively, when an A-MPDU is generated. The purpose of the MD is to delimit the MPDUs within the aggregate. The padding octets are appended to make each MD+MPDU a

multiple of 4 octets in length. The receiver hence can easily find the next MD when transmission error occurs.

Each field in the MD with the corresponding description is listed in Table I. The *MPDU length* field specifies the length of the following MPDU in octets and 8-bit CRC contained in the *CRC* field covers the preceding 16 bits (Reserved and MPDU length fields). In order to correctly determine the boundaries between two consecutive MPDUs, a *unique pattern* is used and the pattern is set to the ASCII value for character 'N.'

The current 802.11n draft specifies the maximum A-MPDU length as 65, 535 bytes. Therefore, a number of MPDUs can be aggregated up to the limit of A-MPDU length within a TXOP limit. Since PHY has no knowledge of MPDU boundaries, such multiple MPDUs form a single PSDU as illustrated in Fig. 1(c). The receiver of an A-MPDU checks the MD for validity based on CRC. If the MD is valid, the corresponding MPDU is extracted from the aggregate. The next MD is expected at the first multiple of 4 octets right after the current MPDU. This extraction process continues until the end of the entire A-MPDU is reached. If the MD is not valid, the receiver skips forward 4 octets and checks if the new location contains a valid MD. Note that the unique pattern is used to reduce the computation required while scanning for a valid MD. It checks the CRC only when the match of the unique pattern is discovered.

Because of the multiple-MPDU aggregation, medium access overhead such as inter-frame spaces and PHY header/preamble is reduced, and medium access efficiency increases. Fig. 1(c), which illustrates A-MPDU frame exchange, shows such reduced overhead compared with other MAC protocols.

D. The 802.11a PHY

In this paper, we use IEEE 802.11a PHY to fairly compare all three MAC protocols, even though the current 802.11n draft specifies higher speed transmission schemes. In 802.11 WLAN, a PHY preamble and a PHY header are attached to a PSDU, and then a PPDU (PHY Protocol Data Unit) is generated as a result. The attached PHY components are illustrated at the front end of an MPDU in Fig. 1.

The 802.11a PHY is based on OFDM (Orthogonal Frequency Division Multiplexing), and provides 8 PHY rates with different modulation and coding schemes at the 5 GHz band [21], as shown in Table II.

There is a trade-off between transmission rate and distance in wireless communications. The eight different rates in the 802.11a PHY also have such a property that higher rates suffer from shorter transmission range, while the throughput-limited lower rates show longer transmission range as illustrated in Fig. 2. This is the reason why any rate adaptation is needed to overcome the rate-distance trade-off. In [22], the authors discovered that the 9 Mbps rate does not show any better propagation property than the 12 Mbps rate, and it is also noticed in Fig. 2. We therefore exclude 9 Mbps rate from the candidate rate set during our simulations in Section V.

The mechanism for the PHY to determine whether the channel is busy or idle is *Clear Channel Assessment* (CCA).

---

[3]There are two types of BACK procedures in the 802.11e, namely, *immediate BACK* and *delayed BACK*. The former is explained and used in this paper as it is a more efficient option [12].

[4]A QoS requirement for a frame is categorized into a *TID* (Traffic Identifier) and is indicated in a corresponding field of the frame header.

PHY Rate	Modulation	Code Rate	BpS*
6 Mbps	BPSK	1/2	3
9 Mbps	BPSK	3/4	4.5
12 Mbps	QPSK	1/2	6
18 Mbps	QPSK	3/4	9
24 Mbps	16-QAM	1/2	12
36 Mbps	16-QAM	3/4	18
48 Mbps	64-QAM	2/3	24
54 Mbps	64-QAM	3/4	27

* Bytes per OFDM Symbol.

The 'CCA busy' is declared by the underlying PHY when the energy level measured at the antenna front-end is above a threshold and/or a known carrier is detected. After detecting a busy channel, a transmitter stops its backoff procedure to avoid a collision.

III. RATE ADAPTATION SCHEMES

As addressed in Section II-D, a rate adaptation scheme should be employed for a multi-rate WLAN to balance the tradeoff between transmission rate and distance. There have been studies on rate adaptation in the 802.11 WLANs. A transmitter can change its transmission rate with or without feedback from the receiver, where the feedback information is typically the desired transmission rate determined by the receiver. Depending on whether they use the feedback from the receiver, rate adaptation schemes are classified into two categories: *closed-loop* and *open-loop* approaches.

With open-loop approaches, a transmitter makes the rate adaptation decision solely based on its local ACK information. As described in Section II-A, an immediate ACK is transmitted by the receiver upon the successful reception of a data frame in the DCF. Open-loop approaches do not require any additional interaction between the transmitter and the receiver, and hence they are standard-compliant.

ARF [14] is the representative open-loop rate adaptation scheme. ARF was originally developed for Lucent Technologies' WaveLAN-II WLAN devices. ARF is the most widely accepted rate adaptation scheme in the 802.11 market. It alternates the transmission rates by keeping track of a timing function as well as missing ACK frames. If two consecutive ACKs are not received correctly by the transmitter, the second retry of the data frame and the subsequent transmissions are made at a lower transmission rate and a timer is started. When either the timer expires or the number of successfully received ACKs reaches 10, the transmission rate is raised to the next higher transmission rate and the timer is restarted unless the new transmission rate is the highest rate. When the transmission rate is the highest, the timer is canceled. However, if an ACK is not received for the very next data frame, the transmission rate is lowered again and the timer is restarted.

ARF is conservative and it does not react quickly when the wireless channel condition fluctuates. The transmitter increases or decreases its transmission rate based on ACK reception without considering the cause of the transmission failures, i.e., channel errors or frame collisions. However, because of its simplicity, ARF is still widely employed in commercial 802.11 WLAN devices and many proposed open-loop rate adaptation schemes, e.g., [23]–[25], are based on ARF.

With closed-loop approaches, the receiver specifies its desired transmission rate and feeds it back to the transmitter. The transmitter then adapts its transmission rate accordingly. Since the rate adaptation is dictated by the receiver, this approach can make a more accurate rate decision in a time-varying wireless channel compared with the open-loop schemes. However, to support such a feedback loop, the format of the frames such as the CTS (and possibly RTS) must be modified or a new field should be added in the MAC header to convey the extra information, which does not conform to the original 802.11 standard.

RBAR [15] is a well-known closed-loop rate adaptation scheme. With RBAR, a transmitter modifies the RTS frame to convey the length information of the subsequent data frame. A receiver estimates the achievable highest transmission rate based on the measured SNR and the conveyed length information. The rate information is fed back to the transmitter with the modified CTS frame. In the current 802.11n draft, a closed-loop rate adaptation scheme is also specified, while other 802.11 standards do not include any rate adaptation scheme. The importance of rate adaptation in WLANs to achieve high capacity is realized by and reflected in the 802.11n standardization.

There are two major differences between RBAR and 802.11n rate adaptation. The first distinctive feature is the different types of carrier frames in which the estimated rate is conveyed. Instead of modifying an existing MAC header field as in RBAR, 802.11n defines a new field *HT (High Throughput) Control Field*. The HT Control Field can be included in any frame. Therefore, a closed-loop rate adaptation can be done without the RTS/CTS frame exchange in the 802.11n rate adaptation scheme.

Second, a transmitter with the 802.11n rate adaptation does not provide the length of the subsequent data and the receiver does not take the length into account for the rate estimation. Therefore, RBAR can make a better rate adaptation decision than the 802.11n rate adaptation. One reason the data length is not considered in the current 802.11n draft is the variable-length MPDUs which can be aggregated into a single PSDU with A-MPDU. On the other hand, RBAR can utilize the MPDU length since a single MPDU is transmitted after the successful RTS/CTS exchange. Consequently, a conservative SNR thresholds has to be used in the 802.11n rate adaptation when the receiver estimates the transmission rate solely based on SNR.

Fig. 2 illustrates the SNR bounds which are used in our 802.11n rate adaptation model. Eight different curves show the throughput performance of 802.11a PHY rates. The maximum MSDU size (i.e., 2304 bytes) is considered to conservatively determine the SNR thresholds. Based on this result, we select
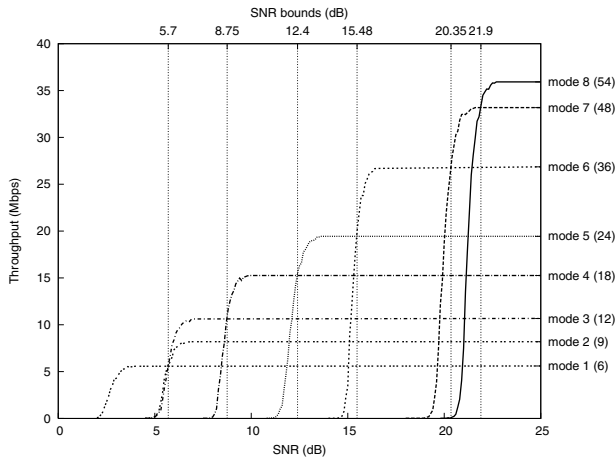
Fig. 2. SNR bounds for 802.11n rate adaptation with the maximum MSDU size (2304 bytes).

six SNR-threshold values at which two or more throughput curves are crossed and the highest transmission rate among the possible rate(s) at the given SNR is selected.

IV. ROUTING METRICS

As routes are typically multi-hop, the performance of wireless mesh networks heavily depends on routing. A routing metric must be carefully chosen to construct high-throughput end-to-end paths. Recent proposals focus on deriving routing metrics that reflect wireless link quality. We employ ETT (Expected Transmission Time) [17] as the metric since its value is adjusted based on different transmission rates. ETT, which is based on ETX (Expected Transmission Count) [16], was designed to reflect varying transmission rate capabilities into the routing metric. Although a recent study showed that ETX gives good performance [19], it considers only the lowest transmission rate (i.e., 1 Mbps) of the 802.11b PHY.

The ETX of a link is the estimated number of data transmissions required to successfully send a packet over that link, including retransmissions. The derivation of ETX starts with measuring the forward and reverse packet delivery ratios of the link. The forward delivery ratio (d_f) is the measured successful transmission probability of a data packet received by the recipient. The reverse delivery ratio (d_r) is the successful transmission probability of an ACK packet measured by the data packet sender. Therefore, the successful transmission probability that a transmission is correctly received and acknowledged is $d_f \times d_r$. Assuming that each transmission is independent from previous transmissions, each transmission attempt including retransmission can be considered a Bernoulli trial, and hence the expected transmission count is given by

$$\text{ETX} = \frac{1}{d_f \times d_r}.$$

ETT is a *bandwidth-adjusted* ETX, and is generated by multiplying the link bandwidth to obtain the time spent in transmitting the data packet. ETT has the form of

$$\text{ETT} = \text{ETX} \times \frac{S}{R},$$

where S denotes the size of the data packet and R is the raw data transmission rate of the link.

V. COMPARATIVE EVALUATION

A. Simulation Setup

We have modified the *ns*-2 simulator [26] by enhancing the original 802.11 DCF module to support 802.11e EDCA with BACK, 802.11n A-MPDU, and 802.11a PHY. In addition, we have also implemented ARF, RBAR, and the 802.11n rate adaptation schemes.

In order to fairly compare all testing schemes, we enable the RTS/CTS exchange for all simulation runs. All control frames such as ACK, RTS, and CTS are transmitted at the lowest transmission rate, 6 Mbps. According to the 802.11 standard, the basic rate should be chosen as the highest one among the transmission rates defined in basic rate set as long as the selected basic rate is lower than or equal to the data transmission rate. However, hidden nodes can easily exist in multi-hop wireless networks, we force mesh nodes to transmit all control frames at the lowest transmission rate. Each source node transmits with 20 dBm transmission power and all mesh nodes are static. The background noise level is set to -93 dBm. We use a log-distance path-loss model with the path-loss exponent of four [27] in AWGN (Additive White Gaussian Noise) channel to simulate the indoor mesh environment. As observed in [28], CS (Carrier Sense) range of the 802.11a PHY is completely covered by the RTS/CTS transmission range. We hence set the CS range to the same range of the RTS/CTS transmission (39.5 meters) in our simulations.

We conduct the simulations under various mesh topologies. Each source node transmits in a saturated mode, i.e., its data queue is never empty. We use LLC/IP/UDP (IEEE 802.2 Logical Link Control/Internet Protocol/User Datagram Protocol) as the upper layer protocol suite, and the MPDU length is fixed at 1024 bytes.

We disable the timer operation of ARF in our simulations as we run a saturated traffic where the packet interarrival time is much shorter than the practical ARF timeout value (i.e., 1 second).

B. Evaluation Framework

All rate adaptation schemes can not be employed for all MAC protocols. For example, the immediate ACK-based ARF
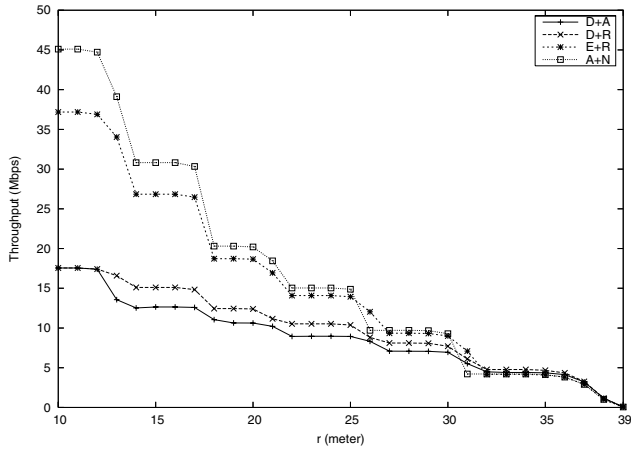
TABLE III
FOUR COMBINATIONS OF MAC PROTOCOLS AND RATE ADAPTATION SCHEMES.

Testing schemes	Abbreviations
DCF + ARF	$D + A$
DCF + RBAR	$D + R$
EDCA with BACK + RBAR	$E + R$
A-MPDU + 802.11n rate adaptation	$A + N$

Fig. 3. Throughput in one-hop topology networks with varying link distance (r).

Fig. 4. Aggregate throughput in three-node ($N = 3$) chain topology networks with varying link distance (r).

works well with a stop-and-wait ARQ. However, ARF would not work well with a BACK scheme, which is provided by 802.11e and 802.11n standards, as it is a selective ARQ. Moreover, the current 802.11n draft specifies its compatible rate adaptation scheme, and hence it is expected that A-MPDU works with the 802.11n rate adaptation instead of with other rate adaptation schemes. Accordingly, we here compare four different combinations of MAC protocols and suitable rate adaptation schemes. The combinations, as listed in Table III, are: (1) DCF + ARF (referred to as $D+A$); (2) DCF + RBAR (referred to as $D + R$); (3) EDCA with BACK + RBAR (referred to as $E + R$); and (4) A-MPDU + 802.11n rate adaptation (referred to as $A + N$). We compare the end-to-end throughput of these schemes.

We use ETT as a routing metric for the reason that ETT is a bandwidth-aware routing metric, which is essential in multi-rate networks. Moreover, ETT was designed for a single-radio wireless mesh network, which is what we consider in this paper. Since we focus on studying the interactions of MAC strategies, we use a pre-computed fixed routing protocol [29]. In our simulation model, each mesh node calculates ETX values between its neighbors and itself based on distances and given path-loss model. ETT is then calculated by using the packet size and the transmission rate. We assume that all mesh nodes have the metric information of all links in the networks, and hence a source node can calculate the Cumulative ETT (CETT) – a sum of ETT values of the end-to-end route – to any destination node. Although we admit this routing protocol is not practical, it will show the performance upper-bound of the ETT metric.

C. One-Hop Topology

We first compare the schemes in the simple one-to-one topology. One source node continuously transmits packets to the other node with various link distance r ($10 \leqslant r \leqslant 39$) meters between the two mesh nodes. Simulation results are plotted in Fig. 3.
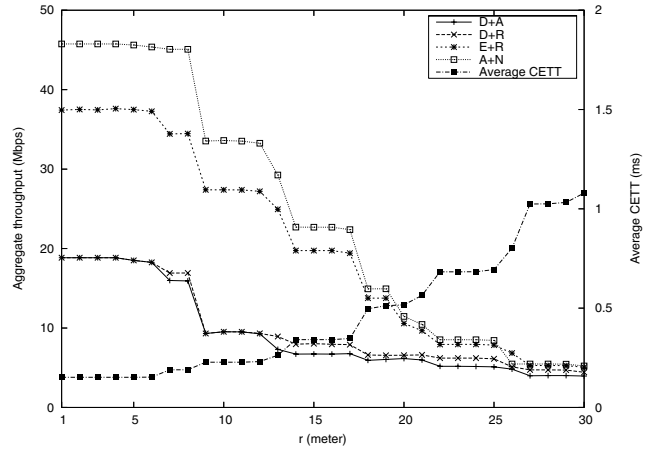
In general, the throughput decreases for all schemes as r increases. We observe that $A + N$ performs the best for a given r except for rate transition points at 26-meter and 31-meter distances. As addressed in Section III, the length of transmitted packets is not taken into account in the 802.11n rate adaptation, and hence we conservatively choose SNR thresholds based on the maximum MSDU size (2304 bytes). This property makes the protocol simple, but less accurate than RBAR, which selects a transmission rate considering the length of the subsequent data packet. Therefore, $A + N$ shows lower throughput than schemes using RBAR at 26 and 36 meters. While all testing schemes achieve comparable throughput in the lowest transmission rate (6 Mbps) range ($32 \leqslant r \leqslant 39$), $D + R$ and $D + A$ show higher performance than the other two schemes. As the TXOP limit in $E + R$ and $A + N$ is set to 3008 μsec and the MSDU size is 1024 bytes, more than one MPDU cannot be transmitted with the TXOP limit when the transmission rate is set to the lowest 6 Mbps. In other words, $E + R$ and $A + N$ suffer from additional overhead of BACK/BREQ frames exchange when only a single MPDU is transmitted during a TXOP.

As also observed in [15], $D + R$ achieves a greater throughput than $D + A$ in the distance range of $13 \leqslant r \leqslant 31$. ARF spends the channel occupancy time in probing the wireless channel condition to increase the transmission rate upon consecutive successful ACK receptions. On the other hand, a transmitter with RBAR need not probe the current channel status as it already has the available highest transmission rate information from the receiver via using the modified RTS/CTS frames exchange.

D. Multi-Hop Chain Topology

We now consider the multi-hop chain-topology networks with varying link distance r ($1 \leqslant r \leqslant 30$) between the adjacent mesh nodes. We also vary the number of nodes (N) from 3 to 5. With a given chain topology, all the participating nodes become traffic sources except one end node, which works as

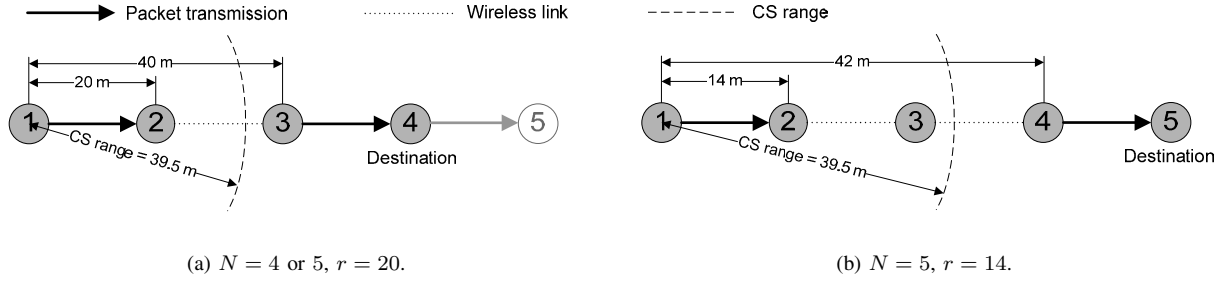(a) $N = 4$ or 5, $r = 20$.

(b) $N = 5$, $r = 14$.

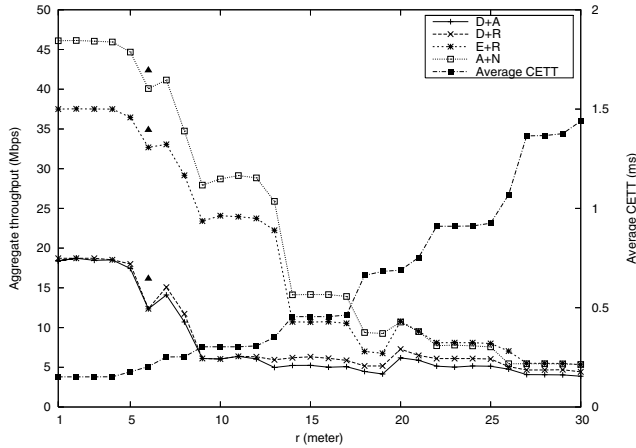Fig. 7. Examples of the spatial reuse in chain-topology networks.

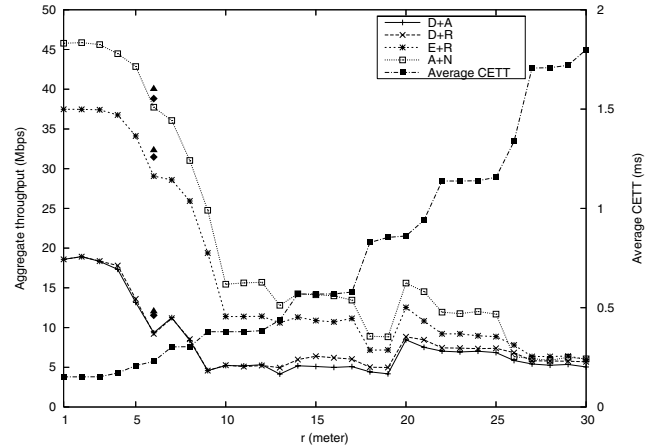Fig. 5. Aggregate throughput in four-node ($N = 4$) chain topology networks with varying link distance (r).

Fig. 6. Aggregate throughput in five-node ($N = 5$) chain topology networks with varying link distance (r).

the destination.

Simulation results in three, four, and five-node chain-topology networks are plotted in Figs. 4, 5, and 6, respectively, along with the corresponding average CETT values. We observe that the end-to-end aggregate throughput decreases, while average CETT increases, as r or N increases in general. However, we observe throughput fluctuations from all testing schemes. Since ETT was designed as a high throughput metric, we expected to see a linear decrease of throughput as CETT increases. Based on our chain-topology results with ETT and CETT, we address two limitations of existing route metrics and routing protocols: being (1) agnostic to spatial reuse and (2) unaware of MAC overhead.

ETT is a well-designed link-quality metric that represents the link reliability and available bandwidth while considering multiple transmission rates. However, most work [16], [17] suggests adding the link metric value of each link along the end-to-end path for the route selection. This algorithm, although simple, does not take into account the spatial reuse and hence fails to take full advantage of available channel capacity of the multi-hop mesh networks. As examples illustrate in Fig. 7, concurrent transmissions are possible, when the end-to-end route is longer than three hops and the distance between

two nodes that are separated by two or more hops is longer than 39.5 meters (CS range). The first example in Fig. 7(a) shows that when $N = 4$ (or $N = 5$) and $r = 20$, node 3 (or node 4) can send packets to its neighbor during the transmission from node 1. When $N = 5$ and $r = 14$, the first and the fourth hops can transmit concurrently as shown in Fig. 7(b). If a route metric such as CETT or an applied routing protocol is designed to take advantage of such spatial reuse, it might make higher-throughput route decisions.

The second issue is that ETT and in turn CETT have no knowledge of underlying MAC protocols. In order to investigate the behavior of (C)ETT, we cross-checked the number of hops with the achieved aggregate throughput in the chain-topology networks. Fig. 8 shows the varying number of hops across the end-to-end route as the distance between adjacent nodes varies. In this figure, N stands for the number of nodes (including the sender itself and the destination), which constitute a route. We observe that all testing schemes show transient throughput fluctuation when the hop count changes. For example, in Fig. 5 ($N = 4$), aggregate throughput results of all testing schemes at $r = 6$ are lower than those of vicinities (i.e., $r = 5$ and $r = 7$). This is because based on CETT one-hop routes are used when $r = 5$ and $r = 7$,
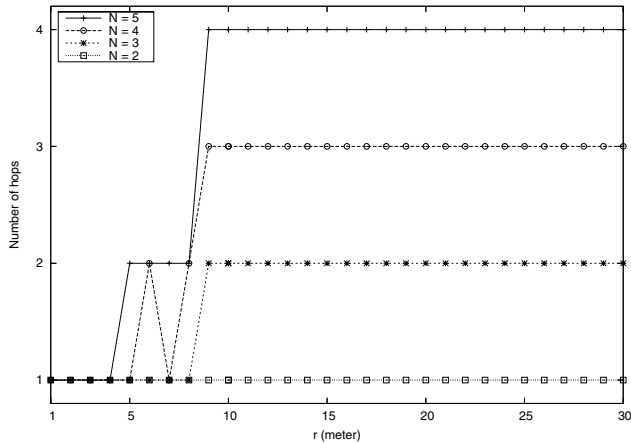
Fig. 8. Comparison of the number of hops in chain topology with varying link distance (r) and the number of nodes (N).

Fig. 9. Average throughput in chain topology over all link distance range r ($1 \leqslant r \leqslant 30$) with the varying number of nodes (N).

while a two-hop route is chosen at $r = 6$. In other words, the two-hop route, i.e., $1 \mapsto 2 \mapsto 4$ (referring to Fig. 7(a)), has a smaller CETT value than the one-hop route, $1 \mapsto 4$, at $r = 6$. However, when we re-run the four testing schemes at $r = 6$ with one-hop route, we obtain higher aggregate throughput performance (illustrated as triangle points in Fig. 5) than the original results based on CETT.[5]

We also have a similar observation from Fig. 6 at $r = 6$. In this environment, both nodes 1 and 2 have two-hop routes (i.e., $1 \mapsto 3 \mapsto 5$ and $2 \mapsto 3 \mapsto 5$, respectively). However, lower aggregate throughput results are observed at $r = 6$ (similar to those in Fig. 5). We re-run simulations with one-hop routes (i.e., $1 \mapsto 5$ and $2 \mapsto 5$) for $A + N$, and obtain higher aggregate throughput performance with such manually configured single-hop routes. The results are illustrated with the following symbols in Fig. 6:

- *Diamond point* (♦): aggregate throughput when $2 \mapsto 5$ route is employed instead of the CETT-based two-hop route.
- *Triangle point* (▲): aggregate throughput with $1 \mapsto 5$ and $2 \mapsto 5$ routes are employed.

For the other schemes (i.e., $D+A$, $D+R$, and $E+R$), we re-run simulations with the single-hop routes, and observe similar aggregate throughput increments as shown in the figure.

These findings raise the need for a new routing metric. As different MACs operate differently, a single metric such as ETT (or CETT) might not select the optimal link and route for all MACs. Accordingly, in a wireless mesh network with the emerging MAC protocols, a new cross-layer metric might be needed to make the applied metric be MAC-aware.

We compare the average aggregate throughput of the schemes over all link distances in Fig. 9. $A + N$ shows the best throughput for all cases of N. The throughput differences between $A+N$, $E+R$, and $D+R$ are due to the different MAC

---

[5]Since the regenerated one-hop results of $D + R$ and $D + A$ are almost the same at $r = 6$, the throughput results of $D + R$ are only shown in Figs. 5 and 6.
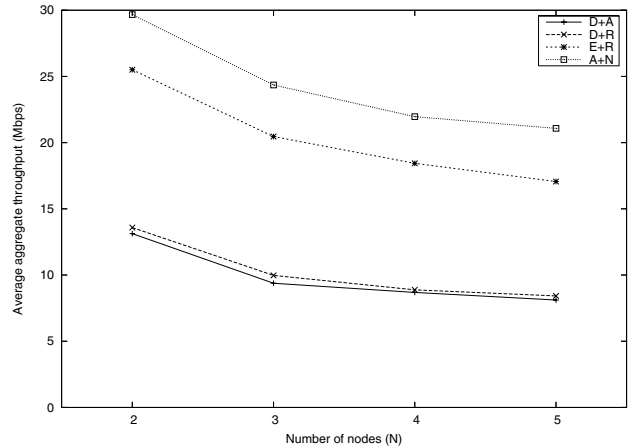
efficiency. $D + A$ shows the lowest performance because ARF consumes channel to probe the wireless channel condition for transmission rate adaptation. The throughput of $A + N$ is about three times that of $D + R$ with $N = 5$, while it is about two times with $N = 2$. We learn that the efficiency of $A + N$ over $D + R$ improves as the number of hops increases. Moreover, this result also implies that the emerging 802.11e/n MACs are effective protocols in multi-hop wireless mesh networks.
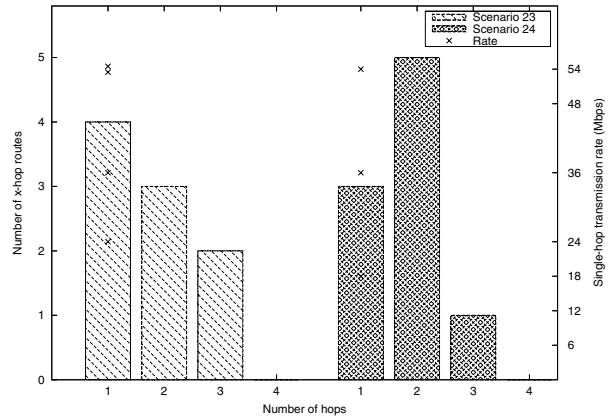
E. Random Topology

We evaluate and compare the performances of the testing schemes in randomly generated network topologies. Within a 30×30 m^2 area, 10 mesh nodes are randomly placed. A gateway node is located in the right upper corner of the area. In each scenario, all mesh nodes (except the gateway) generate traffic. We simulate 40 different scenarios, and the results are plotted in Fig. 10(a). The left and the right y-axes in Fig. 10(a) represent the aggregate network throughput and the average hop counts, respectively. We observe that the schemes with A-MPDU and EDCA with BACK achieve greater throughput than other schemes. We also see that $A + N$ always shows the best throughput for all simulated scenarios. Average aggregate throughput results are summarized in Table IV.

It is interesting that the throughput performance is not proportional to the average hop counts. The maximum longest hops is four at any scenario and all random topologies have approximately 2-hop route on average. However, the throughput performance of all testing schemes do not have a direct relationship with the average hop count. In order to investigate such results, we look into node positions, corresponding hop counts, and the transmission rate of each link in scenarios 23 and 24, which have a large throughput gap in spite of the same average hop count, 1.78. Fig. 10(b) illustrates the hop count distribution (represented by the left y-axis) and the transmission rates of single-hop routes (indexed by the right y-axis) in each scenario. While both scenarios have the same average hop count, we see different hop-count distributions.
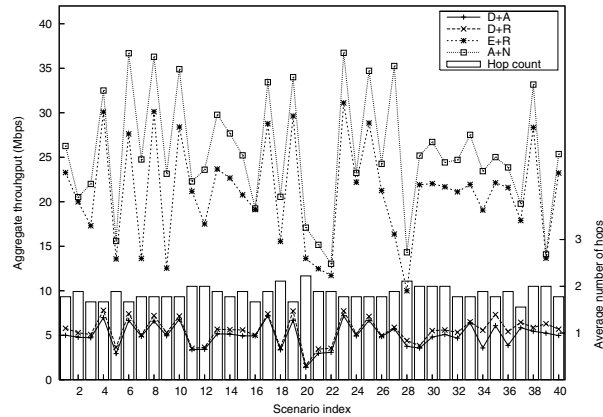
(a) Aggregate throughput of 40 random scenarios.

(b) Hop-count distribution of scenarios 23 and 24.

Fig. 10. Aggregate throughput and hop-count distribution of random-topology networks.

TABLE IV
AVERAGE THROUGHPUT COMPARISON OF FOUR TESTING SCHEMES IN
RANDOM-TOPOLOGY NETWORKS.

	$D+A$	$D+R$	$E+R$	$A+N$
Throughput (Mbps)	4.97	5.52	20.94	25.39

In Fig. 10(b), we observe that different number of single-hop paths and the transmission rates from both scenarios. In scenario 23, there were more single-hop paths and faster links than in scenario 24, and in consequence aggregate A+N throughput was 13.49 Mbps larger in scenario 23. Similar throughput gap is observed in $E + R$ for both scenarios. We believe these throughput gaps result from *temporal fairness* provided by TXOP. As observed in [30], TXOP specified in the 802.11e standard provides temporal fairness among contending nodes, and hence minimizes *performance anomaly* that was first discovered experimentally by the authors of [31]. The performance anomaly phenomenon happens in the following situation: based on randomly generated locations and considered rate adaptation scheme, each contending node may have different transmission rates in a given random topology. Since the 802.11 DCF is designed to offer equal long-term transmission opportunities (or long-term equal medium access probabilities) to all contending nodes, the throughput of a high-rate node is always bounded below the lowest transmission rate irrespective of the transmission-rate diversity in the network. However, the employed TXOP in $E + R$ and $A + N$ can make use of the transmission-rate diversity (i.e., the higher transmission rate, the more chances to transmit packets in a given TXOP limit), and hence can minimize the performance anomaly effect. Consequently, a random scenario which has more high-rate single paths can achieve a higher aggregate throughput performance than other scenarios.

F. Summary

We summarize the key observations from our simulation results as follows:

- $A + N$ and $E + R$ show better performance than other schemes. The performance gain increases as the number of path length increases. We believe the new MAC and rate adaptation features provide good solutions in achieving high wireless mesh backbone capacity.
- Although ETT works well with the emerging MAC protocols in providing high end-to-end throughput, ETT does not generate the optimal throughput when it coexists with A-MPDU and EDCA with BACK. We argue that the routing metrics should consider different MAC features to fully utilize the merits of the enhanced MAC protocols in multi-hop wireless mesh networks. For this purpose, a cross-layer design is required to make the metric be aware of the underlying MAC features. Moreover, we argue that routing protocols should consider spatial reuse which would further increase the capacity of the multi-hop wireless backbone.
- The 802.11n showed poor performance in certain scenarios because its rate adaptation does not consider packet lengths. Although it is difficult to accurately estimate the packet size as various sizes of MPDUs can be aggregated into an A-MPDU, one possible solution is to use the largest MPDU size to estimate the available transmission rate.

VI. CONCLUSION AND FUTURE WORK

We studied the impact of MAC strategies on the capacity of multi-hop wireless mesh networks. We combined the channel access techniques (802.11 DCF, 802.11e EDCA with BACK, and 802.11n A-MPDU) with the rate adaptation algorithms (ARF, RBAR, and 802.11n rate adaptation), along with the ETT routing metric and simulated the performance in various mesh network topologies. We discovered that when worked

together with the proper rate adaptation algorithms, emerging new MAC standards perform well in multi-hop environments. We also discussed the need to design new routing metrics and protocols that will fully utilize the underlying MAC features.

Our ongoing work includes formulating a cross-layer metric that accurately estimates and incorporates channel access overhead of different MAC protocols. We are building a testbed network to investigate the performance of the protocols in a real network in addition to our simulations. We will keep track of standardization activities of 802.11e/n/s and improve the wireless mesh network performance with the new features.

REFERENCES

[1] I. F. Akyildiz, X. Wang, and W. Wang, "Wireless Mesh Networks: A Survey," *Computer Networks Journal*, vol. 47, pp. 445–487, 2005.

[2] R. Bruno, M. Conti, and E. Gregori, "Mesh Networks: Commodity Multihop Ad Hoc Networks," vol. 43, no. 3, pp. 123–131, Mar. 2005.

[3] Seattle Wireless. [Online]. Available: http://www.seattlewireless.net/

[4] MIT Roofnet. [Online]. Available: http://pdos.csail.mit.edu/roofnet/

[5] MSR: Self-Organizing Neighborhood Wireless Mesh Networks. [Online]. Available: http://research.microsoft.com/mesh/

[6] Mesh Dynamics. [Online]. Available: http://www.meshdynamics.com/

[7] Tropos Networks. [Online]. Available: http://www.tropos.com/

[8] Champaign-Urbana Community Wireless Network. [Online]. Available: http://www.cuwireless.net/

[9] P. Kyasanur, J. So, C. Chereddi, and N. H. Vaidya, "Multi-Channel Mesh Networks: Challenges and Protocols," vol. 13, no. 2, pp. 30–36, Apr. 2006.

[10] P. Bahl, A. Adya, J. Padhye, and A. Wolman, "Reconsidering Wireless Systems with Multiple Radios," *ACM SIGCOMM Computer Communication Review (CCR)*, vol. 34, pp. 39–46, Oct. 2004.

[11] IEEE 802.11, *Part 11: Wireless LAN Medium Access Control (MAC) and Physical Layer (PHY) specifications*, IEEE Std. 802.11-1999, Aug. 1999.

[12] IEEE 802.11e, *Part 11: Wireless LAN Medium Access Control (MAC) and Physical Layer (PHY) specifications: Medium Access Control Quality of Service Enhancements*, Supplement to IEEE Std. 802.11, Sept. 2005.

[13] IEEE 802.11n/D1.0, *Part 11: Wireless LAN Medium Access Control (MAC) and Physical Layer (PHY) specifications: Enhancements for Higher Throughput*, Draft Supplement to IEEE Std. 802.11, Draft 1.0, Mar. 2006.

[14] A. Kamerman and L. Monteban, "WaveLAN-II: a high-performance Wireless LAN for the Unlicensed Band," *Bell Labs Technical Journal*, vol. 2, no. 3, pp. 118–133, Aug. 1997.

[15] G. Holland, N. Vaidya, and P. Bahl, "A Rate-Adaptive MAC Protocol for Multi-Hop Wireless Networks," in *Proc. ACM MobiCom*, Rome, Italy, July 2001, pp. 236–251.

[16] D. S. J. De Couto, D. Auayo, J. Bicket, and R. Morris, "A High-Throughput Path Metric for Multi-Hop Wireless Networks," in *Proc. ACM MobiCom*, San Diego, CA, USA, Sept. 2003, pp. 134–146.

[17] R. Draves, J. Padhye, and B. Zill, "Routing in Multi-Radio, Multi-Hop Wireless Mesh Networks," in *Proc. ACM MobiCom*, Philadelphia, PA, USA, Sept. 2004, pp. 114–128.

[18] J. Bicket, D. Aguayo, S. Biswas, and R. Morris, "Architecture and Evaluation of an Unplanned 802.11b Mesh Network," in *Proc. ACM MobiCom*, Cologne, Germany, Aug. 2005.

[19] R. Draves, J. Padhye, and B. Zill, "Comparison of Routing Metrics for Static Multi-Hop Wireless Networks," in *Proc. ACM SIGCOMM*, Portland, OR, USA, Sept. 2004, pp. 133–144.

[20] I. Tinnirello and S. Choi, "Efficiency Analysis of Burst Transmissions with Block ACK in Contention-Based 802.11e WLANs," in *Proc. IEEE ICC*, Seoul, Korea, May 2005, pp. 3455–3460.

[21] IEEE 802.11a, *Part 11: Wireless LAN Medium Access Control (MAC) and Physical Layer (PHY) specifications: High-speed Physical Layer in the 5 GHz Band*, Supplement to IEEE Std. 802.11, Sept. 1999.

[22] D. Qiao and S. Choi, "Goodput Enhancement of IEEE 802.11a Wireless LAN via Link Adaptation," in *Proc. IEEE ICC*, Helsinki, Finland, June 2001, pp. 1995–2000.

[23] P. Chevillat, J. Jelitto, A. N. Barreto, and H. L. Truong, "A Dynamic Link Adaptation Algorithm for IEEE 802.11a Wireless LANs," in *Proc. IEEE ICC*, Anchorage, AK, USA, May 2003, pp. 1141–1145.

[24] D. Qiao and S. Choi, "Fast-Responsive Link Adaptation for IEEE 802.11 WLANs," in *Proc. IEEE ICC*, Seoul, Korea, May 2005, pp. 3583–3588.

[25] J. Kim, S. Kim, S. Choi, and D. Qiao, "CARA: Collision-Aware Rate Adaptation for IEEE 802.11 WLANs," in *Proc. IEEE INFOCOM*, Barcelona, Spain, Apr. 2006.

[26] The Network Simulator – *ns*-2. [Online]. Available: http://www.isi.edu/nsnam/ns/

[27] T. S. Rappaport, *Wireless Communications: Principle and Practice*, 2nd ed. Prentice-Hall, 2002.

[28] D. Qiao, S. Choi, A. Jain, and K. G. Shin, "MiSer: An Optimal Low-Energy Transmission Strategy for IEEE 802.11a/h," in *Proc. ACM MobiCom*, San Diego, CA, USA, Sept. 2003, pp. 161–175.

[29] A. Raniwala and T. cker Chiueh, "Architecture and Algorithms for an IEEE 802.11-Based Multi-Channel Wireless Mesh Network," in *Proc. IEEE INFOCOM*, Miami, FL, USA, Mar. 2005, pp. 2223–2234.

[30] I. Tinnirello and S. Choi, "Temporal Fairness Provisioning in Multi-Rate Contention-Based 802.11e WLANs," in *Proc. IEEE WoWMoM*, Taormina, Italy, June 2005, pp. 220–230.

[31] M. Heusse, F. Rousseu, G. Berger-Sabbatel, and A. Duda, "Performance Anomaly of 802.11b," in *Proc. IEEE INFOCOM*, San Francisco, CA, USA, Mar. 2003, pp. 836–843.